Lidar-based height correction for the assimilation of atmospheric motion vectors

Kathrin Folger and Martin Weissmann

Hans-Ertel-Centre for Weather Research, Data Assimilation Branch, Ludwig-Maximilians-Universität, Munich, Germany

Manuscript for submission to the *Journal of Applied Meteorology and Climatology*

September 2015

Corresponding author address:

Kathrin Folger

LMU Meteorologie

Theresienstraße 37

80333 Munich, Germany

E-Mail: kathrin.folger@lmu.de

Abstract

The study uses lidar observations from the polar orbiting *Cloud–Aerosol Lidar and Infrared Pathfinder Satellite Observations* (CALIPSO) satellite to correct operational atmospheric motion vector (AMV) pressure heights. This intends to reduce the height assignment error as well as the horizontal error correlation of AMVs for their use in data assimilation. Additionally, AMVs are treated as winds in a vertical layer as proposed by several recent studies. Corrected and uncorrected AMV winds are evaluated using short-term forecasts of the global forecasting system of the German Weather Service.

At first, a direct lidar-based height correction of collocated AMV and CALIPSO observations is evaluated. Assigning AMV winds from Meteosat-10 to ~120 hPa deep layers below the lidar cloud top reduces the wind errors of AMVs from Meteosat-10 by 7-15%. In addition, the AMV error correlation is reduced by about 50 km through the correction. However, such a direct correction can only be applied to collocated AMV/CALIPSO observations that exhibit a comparably small subset of all AMVs.

Secondly, CALIPSO observations are used to derive statistical height bias correction functions for a general height correction of all operational AMVs from Meteosat-10. Such a bias correction achieves on average about 50% of the error reduction of the direct correction. Results for other satellites are more ambiguous, but still encouraging. Given that such a bias correction can be applied to all AMVs from a geostationary satellite, the method exhibits a promising approach for the assimilation of AMVs in numerical weather prediction models in the future.

1 Introduction

Atmospheric Motion Vectors (AMVs) are retrievals of the atmospheric wind field derived by tracking cloud and water vapor structures in successive satellite images. These structures characterize tropospheric motions, and thereby the horizontal wind speed and wind direction can be determined. By using imagery from geostationary and polar-orbiting satellites and also exploiting the possibility of combining images from different satellites (Lazarra et al., 2014), AMVs are almost globally available. AMVs provide wind information with a unique spatial and temporal coverage, especially over the oceans and in polar regions with traditionally rare in-situ observations. Given that the current global observing system is heavily skewed towards mass/temperature observations, reliable wind observations in remote areas are an essential data source for global numerical weather prediction (NWP) models (Baker et al., 2014). AMVs are therefore assimilated routinely in all global NWP systems, and many studies showed that this type of satellite data has a positive impact on the forecast skill of NWP models (Bormann and Thépaut, 2004; Velden et al., 2005; Joo et al., 2013).

Although AMVs have proven to be an important source of wind information, some issues still remain. One unsolved problem comprises spatially correlated errors up to horizontal distances of several hundred kilometres (Bormann et al., 2003). The main contributor to the AMV wind error and error correlation is the height assignment, which can be particularly error-prone when the wind varies strongly with height. Velden and Bedka (2009) estimated that 70% of the total AMV wind error arises from height assignment issues. A number of error sources contribute to this: Temperature and humidity model profiles that are used to retrieve the AMV height may contain errors that are often correlated horizontally, and multi-layer clouds or semi-transparent clouds pose a further challenge for the height assignment process. Studies on AMV error characteristics and the improvement of the AMV height assignment are therefore an active field of research (e.g. Borde et al., 2014, Salonen et al., 2014, Bresky et al., 2012).

In practice, these issues lead to a massive thinning of the originally dense AMV dataset for data assimilation. As an example, the German Weather Service (DWD) thins AMVs to a minimum horizontal distance of 200 kilometres in their global NWP system.

AMVs are traditionally interpreted as single level observations. However, recent research revealed that this assumption should be reconsidered. Several studies showed that AMVs rather represent vertical layers instead of discrete levels (Hernandez-Carrascal and Bormann 2014; Weissmann et al. 2013; Velden and Bedka 2009). In Folger and Weissmann (2014), a combined approach of layer-averaged and lidar-corrected AMVs was used to correct AMV pressure heights of Meteosat-9 and -10, verified by nearby operational radiosondes. The aim of the present paper is to further elaborate this concept, and to overcome the limitations of spatially and temporally rare radiosonde observations by using model equivalents for the wind verification. As in Folger and Weissmann (2014), lidar observations from the polar orbiting *Cloud–Aerosol Lidar and Infrared Pathfinder Satellite Observations* (CALIPSO) satellite are used to correct AMV pressure heights. In the first part of the present study, a direct correction of AMVs with collocated CALIPSO observations is evaluated using different layer depths and layer positions relative to the lidar cloud-top height and relative to the operationally assigned AMV height. Furthermore, effects on the AMV error correlation are quantified. In the second part of this study, height bias correction functions for a general height adjustment of operational AMVs are derived to proceed from an individual height correction to a larger scope of application. This approach allows using lidar information for the AMV height correction without the need of real-time lidar data.

2 Data and Method

2.1 Datasets

a) AMVs from geostationary satellites

The study is mainly focused on AMVs derived from images of the European geostationary satellite Meteosat-10, which is located at 0° longitude and covers Europe, Africa and large parts of the Atlantic Ocean. In addition, an overview of results for AMVs from other geostationary satellites that are used routinely in global NWP models is provided. These are Meteosat-7 at 57°E, the *Multi-Functional Transport Satellite 2* (MTSAT-2) at 145°E and the two *Geostationary Operational Environmental Satellites* (GOES) at 135°W (GOES-West) and 75°W (GOES-East). The geographical position of these satellites is shown in Figure 1. Meteosat-10 belongs to the Meteosat Second Generation with in total 12 channels in the visible and infra-red range that can be used for the AMV derivation. Meteosat-7 (Meteosat First Generation) is less sophisticated with only 3 channels and consequently, considerably fewer AMVs are available. Meteosat-AMVs are derived operationally by the *European Organization for the Exploitation of Meteorological Satellites* (EUMETSAT). GOES satellites have 6 channels each and GOES-AMVs are provided by the *National Environmental Satellite Data and Information Service* (NESDIS) of the *National Oceanic and Atmospheric Administration* (NOAA). MTSAT-2 is the Japanese geostationary satellite with 5 channels; MTSAT-2-AMVs are provided by the *Japan Meteorological Agency* (JMA). As Meteosat-7 provides only a small AMV sample and results tend to be similar to Meteosat 10, only results for MTSAT-2-AMVs and for the two GOES satellites combined are shown in addition to a detailed evaluation for Meteosat-10.

AMVs are derived by using images from different satellite channels. Generally, visible channels (VIS) are used in the lower troposphere below pressure heights of 700 hPa during daylight periods. AMVs from infrared channels (IR) are derived throughout the troposphere, whereas AMVs from water vapor channels (WV) are mainly found in upper levels above 600 hPa. WV-AMVs are derived by tracking cloud structures as well as water vapor gradients. As

AMV pressure heights are compared to lidar cloud-top observations in this study, WV-AMVs derived from water vapor structures are not considered. There are several AMV height assignment methods that are used operationally. The *Equivalent Black Body Temperature* (EBBT) method is the most common method for low-level opaque clouds, using brightness temperatures of IR satellite images to retrieve height levels for AMVs. For high-level AMVs, the CO_2-slicing and the H_2O-intercept method both utilize differences of two satellite channels for the height assignment. More details on height assignment methods can be found in Di Michele et al. (2013) and Salonen et al. (2014). Unfortunately, the resulting operational Meteosat-AMV data set contains no information on the height assignment method applied for deriving individual AMVs.

b) Lidar observations from CALIPSO

The polar-orbiting satellite CALIPSO was launched in 2006 as part of the "A-Train" and flies in a sun-synchronous orbit in 705 km altitude, encircling the earth in about 100 minutes. The lidar CALIOP (*Cloud–Aerosol Lidar with Orthogonal Polarization*) on board is currently the only space-borne lidar and thus provides unique information on clouds and aerosols from space. This study uses the level-2 cloud-layer product, which provides information on the lidar cloud-top height with high horizontal (1 km) and vertical resolution. The latter varies for different altitudes: At lower altitudes (-0.5 km to 8.2 km), the vertical resolution is 30 m and at higher altitudes (from 8.2 to 20.1 km) it is 60 m. The combined use of two wavelengths in the visible (543 nm) and IR (1064 nm) range allows retrieving additional information on the specific cloud scene, such as cloud phase or multi-layer cloud situations. Additionally, the *Cloud-Aerosol-Distinguisher* (CAD) is defined as a quality index that indicates the reliability of the retrieved lidar information, ranging from +100 (cloud observation) to -100 (aerosol

observation). For more information on CALIPSO, see Winker et al. (2009, 2010) and Hunt et al. (2009).

c) Collocation of AMVs and lidar observations

In order to find suitable CALIPSO lidar cloud-top observations that are close to AMVs, different collocation criteria are applied that generally follow Folger and Weissmann (2014). For Meteosat-AMVs, the maximum horizontal distance between AMVs and collocated CALIPSO lidar observations was set to 50 km, with a maximum time difference of 30 min. The median of all lidar cloud-top observations within this range is taken as a representative cloud top, which is then compared to the operational AMV pressure height. Thereby, a threshold of at least 20 lidar observations within this range is applied. In addition, the root mean square difference between these lidar observations and their median must be smaller than 70 hPa. Multi-layer cloud scenes as well as cloud observations with a CAD < 90 are discarded. The AMV quality index (ranging from 0 to 100, with 100 indicating the best possible quality) must be greater than 50. However, errors may still arise due to the horizontal and temporal distance, so that different clouds might be observed from lidar and AMV tracking feature. Therefore, only AMVs that are at most 100 hPa above and 200 hPa below the respective median cloud-top heights are considered. This interval is chosen on the assumption that an AMV represents the atmospheric motion of a vertically extended cloud structure and is therefore located below the actual cloud top. All AMVs beyond this range are discarded.

For GOES- and MTSAT-2-AMVs, these collocation criteria are slightly adjusted in order to avoid problems with semi-transparent clouds. First, the AMV quality index threshold is raised from 50 to 80. In addition, AMVs were only used if the CALIPSO flight path approaches the AMV position to less than 10 km, which corresponds to an average distance of ca. 25

kilometres between the AMV and the available lidar cloud-top observations within the 50-km radius that is used for the calculation of the median lidar cloud-top height.

d) Study periods

Two different periods are evaluated in this study. For the evaluation of the direct lidar height correction in Section 3.1, the study period comprises 11 days (31 May – 10 June 2013, first evaluation period) of operational AMVs. For the height bias correction functions in Section 3.2, a 6-day time interval is used that ranges from 7 May to 12 May 2013 (second evaluation period). This slightly different timeframe is chosen because continuous CALIPSO lidar observations are needed in section 3.2 in the preceding 30-day time interval of the respective evaluation period to calculate correction functions. This criterion is not fulfilled for the first evaluation period due to gaps in the CALIPSO data set. Fig. 1 shows the position of AMVs with collocated lidar observations in the second evaluation period.

The study uses high-level AMVs above a pressure height of 400 hPa and low-level AMVs below a pressure height of 700 hPa. As there are traditionally few mid-level AMVs, AMVs between 400 hPa and 700 hPa are not evaluated due to an insufficient sample size. Fig. 2 shows the vertical distribution of AMVs for both evaluation periods for Meteosat-10. Altogether, 13200 AMVs in the first evaluation period and 7410 AMVs in the second evaluation period are analysed, with about 70% of them located in low-level and 30% in high-level regions. For the other geostationary satellites, there are considerably fewer AMVs available. Table 1 lists the numbers of all used AMVs with collocated lidar observations for both periods. Only about 10% of the number of Meteosat-10-AMVs is found for MTSAT-2 and GOES-AMVs. This is due to the smaller number of available AMVs from these satellites, as well as due to the stricter collocation criteria described in the previous paragraph.

2.2 Methods

a) Layer-averaged GME model winds

Several studies showed that AMVs should be interpreted as layer-averages instead of winds at discrete levels. Satellites detect radiation from finite vertical layers and additionally the motion of clouds rather represents a vertically averaged wind over the whole cloud than the wind at the cloud top (Hernandez-Carrascal and Bormann, 2014). Folger and Weissmann (2014) used collocated operational radiosondes to show that layers relative to the lidar cloud top yield an error reduction of 12% (17%) compared to layers (levels) centered at the operational AMV height. The additional need of verification radiosondes massively limits the sample size of collocated AMVs and lidar observations to about one percent of the original number. To overcome this limitation, GME model equivalents are used in this study for the wind verification. GME was the operational global forecasting system of the German Weather Service (DWD) until July 2015, with a horizontal grid spacing of 20 km and 60 levels in the vertical. An observation operator for layer-averaged AMVs was recently implemented at DWD. This operator provides AMV model equivalents derived from short-term (first-guess) forecast that are used for verification. The geographical position of each AMV is horizontally interpolated between the grid points, and then the vertical layer averaging over the respective layer is applied. As the assimilation window of GME is 3 h, the maximum temporal difference between AMV and model equivalents is 90 minutes.

b) AMV height correction with collocated lidar observations

Based on the results of Folger and Weissmann (2014), layers of varying depth ranging from 0 to 200 hPa at three positions are evaluated: (i) below the lidar cloud-top height, (ii) with 25%

above and 75% below the lidar cloud-top height and (iii) centered at the operational AMV height. This is schematically illustrated in Fig. 3. In order to assess the benefit of lidar-corrected and layer-averaged AMVs, two error metrics are applied for all considered layers: The Vector Root Mean Square Error (VRMS), and the wind speed bias. These are calculated as follows:

$$VRMS = \frac{1}{N}\sum_{i=1}^{N}\sqrt{du_i^2 + dv_i^2}$$

$$BIAS = \frac{1}{N}\sum_{i=1}^{N}(windspeed_{\text{oper,i}} - windspeed_{\text{model,i}})$$

with $du_i = u_i(\text{AMV\_operational}) - u_i(\text{AMV\_model})$, dv_i analogously. N is the number of available AMVs with corresponding CALIPSO lidar cloud-top observations, *oper* denotes operational wind values and *model* the GME model equivalents of the respective layers.

c) AMV error correlations

AMVs exhibit significant spatially correlated errors that are caused by several reasons. Height assignment procedures use model temperature profiles that are already correlated mutually. In addition, AMVs that tend to be dissimilar to their neighbours are rejected during quality control processes, thereby enhancing existing error correlations. In this study, error correlations for operational AMVs and for AMVs that are assigned to 120-hPa layer-averages below the lidar cloud-top height are compared. For this purpose, all Meteosat-10-AMVs with available collocated lidar observations during the first evaluation period (31 May – 10 June 2013) are considered (called AMV sample "A" in the following). For these AMVs, circumjacent AMVs (without a direct lidar height correction available, AMV sample "B") are divided into 50-km-bins around each AMV A for the same point in time. In addition, the vertical distance between the AMV pressure heights may not exceed 150 hPa for the obtained

AMV-A/AMV-B pairs. Error correlations for the u-component of the wind field are calculated for each 50-km-bin as follows (analogously for the v-component):

$$operational\_corr(u) = corr((u_{A,oper} - u_{A,model\_oper}),(u_{B,oper} - u_{B,model\_oper}))$$

$$Calipso\_corr(u) = corr((u_{A,oper} - u_{A,model\_Calipso}),(u_{B,oper} - u_{B,model\_oper}))$$

where the index *A* denotes the AMVs with a direct CALIPSO lidar height correction available and *B* the AMVs without collocated lidar observations that surround AMV A . The index *oper* indicates the operationally assigned wind, *model_oper* the model winds at the operational AMV heights, and *model_Calipso* the lidar-corrected and layer-averaged model equivalents. The total error correlation *operational_corr* (u and v combined) is then derived as $0.5 * (operational\_corr(u) + operational\_corr(v))$, with *Calipso_corr* analogously.

d) Height bias correction functions

The previously described direct AMV height correction method is based on actual cloud-top heights of collocated lidar observations of the respective AMV. However, this method is only applicable to a small number of operational AMVs, as time and position of the AMVs have to coincide with nearby CALIPSO lidar observations. As an alternative approach, height bias correction functions are calculated for a general mean adjustment of all AMV heights from a respective satellite. For this purpose, the direct CALIPSO height correction is applied to all available AMVs within a certain timeframe and then an average over the resulting height adjustment values is computed. This height bias correction is then applied to a subsequent independent verification period. Durations of 30 days and 10 days are used as averaging timeframes and the resulting corrections are applied during the second evaluation period (7

May to 12 May 2013). The 30-day mean comprises the days from 1 April to 6 May 2013 (with missing CALIPSO data on six days within this interval). The 10-day mean is calculated from the actual preceding days of the respective date. This means that for example the bias correction derived from the period 2 – 11 May 2013 is applied and evaluated on 12 May 2013. As a third approach, the 30-day period is subdivided to determine separate correction functions for the northern hemisphere (latitude larger than 25°N), the southern hemisphere (latitude larger than 25°S) and a tropical region in between. Table 2 lists the numbers of AMVs with collocated CALIPSO lidar observations that are used for the different height correction periods for Meteosat-10. For the other geostationary satellites (section 3.3), only a 30-day average is calculated for the height bias correction due to the smaller number of available AMVs. The counts for GOES- and MTSAT-2-AMVs are listed in Table 3. Height bias correction functions are calculated for the different channels (VIS, IR and WV) for 50-hPa altitude-bins between 950 hPa and 200 hPa plus one additional bin for AMVs below and above this range, respectively. Every bin must contain at least 30 individual correction values to determine a valid mean adjustment for the respective altitude bin and AMV channel.

Mean VRMS differences and wind speed bias values are calculated for all AMVs (i) for the discrete operational levels, (ii) for levels at 60 hPa below the actual lidar cloud-top observation and (iii) for the adjusted levels based on the height bias correction functions. In addition, 120-hPa-deep layer-averages centered at these levels are considered. The level 60 hPa below the lidar cloud top was chosen as it represents the mean pressure of the 120-hPa layer.

3 Results

The first two sections (3.1 and 3.2) present results for lidar-based height correction methods for the European geostationary satellite Meteosat-10. In 3.1, results on the direct CALIPSO

lidar height correction are shown. Section 3.2 comprises results on height bias correction functions that can be used as a general height adjustment, omitting the need of a directly collocated lidar observation for a single AMV. Section 3.3 provides a brief evaluation of both methods for other geostationary satellites.

3.1 Direct CALIPSO lidar height correction

a) VRMS and wind speed bias

AMV winds are evaluated by assigning AMVs to different layers and levels relative to the original AMV height and relative to the lidar cloud-top height during the first evaluation period (31 May – 10 June 2013). Figure 4 illustrates the distribution of height differences between operational AMV heights and cloud-top heights derived from collocated CALIPSO lidar observations for all used Meteosat-10-AMVs. More than 80% of all operationally assigned AMVs are located below the actual lidar cloud top, corresponding to positive height differences on the x-axis. The highest number of AMVs occurs within the first 50 hPa below the lidar cloud top.

Figure 5 shows the VRMS difference and wind speed bias between operational AMV winds and layer-averaged model winds. Grey dashed lines represent layers that are centered at the operational AMV height, which serve as a reference for the lidar-corrected layers relative to the lidar cloud-top height (black lines). High-level AMVs above a pressure height of 400 hPa comprise WV and IR AMVs, whereas low-level AMVs below a pressure height of 700 hPa consist mainly of VIS and IR AMVs. Dividing the AMVs data set for different channels used for their derivation shows similar results for both high- and low-level AMVs and is therefore not shown.

For high-level AMVs (Fig. 5a), lowest VRMS differences are achieved for 120-hPa layers below the lidar cloud top, resulting in a relative error reduction of about 10% when compared to reference layers of the same depth centered at the original AMV height (dashed line) and of about 15% when compared to the discrete operational AMV heights (dashed line at 0 hPa). The wind speed bias tends to be close to zero for 100-hPa layers below the lidar cloud top. Low-level AMVs (Fig. 5b) show lowest VRMS differences for 120-hPa layers below the lidar cloud top and for 200-hPa layers with 25% above and 75% below the lidar cloud top. For 120-hPa layers below the lidar cloud top, the correction reduces the VRMS difference by 8 % and 15% compared to reference layers centered at the operational AMV height and to the discrete operational height, respectively. The wind speed bias is generally small for low-level AMVs, but layers below the lidar cloud top exhibit slightly smaller values than the 25%/75% layers.

b) AMV error correlations

To investigate the effect of the lidar height correction on the horizontal correlation of AMV errors, correlation coefficients are computed as a function of horizontal distance (Fig. 6). The black, dashed line in Fig. 6 corresponds to the error correlation for AMVs at the operational pressure height, showing a decrease of the correlation with increasing horizontal distance. The grey line represents values for the correlation of lidar-corrected AMVs (using 120-hPa deep layers below the lidar cloud-top height) to operational AMVs. The lidar-corrected data set shows a significantly lower correlation to the operational AMVs which further emphasizes the potential benefit of lidar-corrected AMVs for data assimilation. On average, the lidar-correction reduces the correlation by about 50 km. As the AMV verification is conducted with model equivalents, the absolute values of the correlation are strongly affected by the horizontal correlation of model errors and should not be evaluated. However, the model

correlation can be expected to be independent of the AMV errors and therefore results for the corrected and uncorrected AMV data set can be compared. Bormann et al. (2003) calculated the error correlation of AMVs using radiosondes for verification and found correlation values that were about 30% smaller than the values in Fig. 6. This difference is likely the contribution of the model correlation.

3.2 Height bias correction functions

Folger and Weissmann (2014) and the previous section showed that a direct lidar-based height correction significantly reduces the wind error of AMVs. However, this direct correction can only be applied to a small fraction of the AMV data set, where collocated CALIPSO observations are available for the correction. This section evaluates the potential of general lidar-based height bias correction functions derived from a preceding 10-30 day period, with an additional hemispheric subdivision of the 30-day period. This approach has the advantage that the full operational AMV data set for a respective satellite can be corrected.

The previous section showed that 120-hPa-deep layers below the lidar cloud top yield lowest VRMS differences and wind speed bias values. For this reason, layers of that position and depth and, as discrete levels, 60 hPa levels below the lidar cloud top are used for the calculation of height bias correction functions. Exemplarily, Fig. 7 shows the 30-day lidar-based bias correction for Meteosat-10 as a function of altitude and satellite channel. Negative values indicate that the AMV is shifted downwards in the atmosphere. Mid-level AMVs between 400 hPa and 700 hPa are not used for the height correction given the comparably small AMV density in this range. Generally, the adjustment of high-level AMVs is of the order of minus 20 hPa. Low-level AMVs are also shifted downwards at most altitude levels. The largest adjustment of 60-80 hPa occurs for AMVs in 700-800 hPa altitude. Generally, the

curves of height bias correction functions based on a 10-day mean as well as for the latitude subdivision (both not shown) tend to have a similar shape as the 30-day mean, with less pronounced height adjustment values for the tropics than for the extra-tropics.

Fig. 8 shows the mean VRMS difference and wind speed bias between AMV and model winds for applying the height bias correction to Meteosat-10-AMVs during the second evaluation period (7 May – 12 May 2013). Black bars represent results for operational AMV heights, striped bars for the CALIPSO height correction with directly collocated lidar observations, and grey bars for the three different height bias correction functions. The left part of each panel shows the results for discrete levels (operational levels, levels at 60 hPa below the lidar cloud top and "adjusted" levels based on the three height bias correction functions). Accordingly, the right part represents layer-averaged values for 120-hPa deep layers centered at the respective heights. Results for the direct lidar height correction are generally similar to the results in Section 3.1.a, with slight variations due to the different evaluation periods considered in the two sections.

For high-level AMVs (Fig. 8a), lowest VRMS differences (upper panel) are achieved for 120-hPa layers based on the direct lidar height correction. However, the lidar height bias correction reveals a distinct error reduction compared to levels/layers relative to the operational AMV height and achieves about 30-50% of the reduction of the direct correction, with no clear preference for a particular correction function. In addition, the wind speed bias (lower panel) is clearly reduced for the direct lidar height correction as well as for height bias correction functions based on a 30-day mean and a 10-day mean when compared to the wind speed bias at the operational AMV height.

Low-level AMVs (Fig. 8b) exhibit a similar pattern as high-level AMVs. Again, the direct CALIPSO lidar height correction shows best results when layer-averages are used. In addition, layers relative to the adjusted heights based on the height bias correction show a clear error reduction of VRMS differences compared to the operational values. In particular,

406 the 10-day bias correction exhibits VRMS differences that are almost equally low as errors of
407 the direct lidar height correction. The wind speed bias for low-level AMVs is strongly
408 reduced for the direct lidar height correction as well as for the height bias correction,
409 especially when a layer-averaging at the respective height is applied. Overall, VRMS
410 differences are generally lower for layer-averages than for discrete levels, which further
411 emphasizes that AMVs represent the wind in a vertically extended layer.
412 To investigate the effect of different layer depths and level positions relative to the lidar
413 cloud-top height, Fig. 9 shows the relative reduction of VRMS differences of both lidar height
414 correction methods (direct lidar correction and lidar-based bias correction) for discrete levels
415 and finite layers when their results are compared directly to the results for the discrete
416 operational AMV heights. Relative error reduction values are shown as a function of layer
417 depth for low- and high-level AMVs combined. Solid lines correspond to layers/ levels of the
418 direct lidar height correction, whereas dashed lines represent layers/levels relative to the
419 adjusted height based on a 30-day bias correction. Overall, best results are achieved by the
420 direct lidar height correction for 120-hPa layers below the lidar cloud top (solid black line)
421 with an error reduction of about 11% compared to the operational AMV heights. Again, this
422 value deviates slightly from the error reduction found in section 3.1 (~ 15%), as two different
423 evaluation periods are considered in the two sections. Using the bias correction, the largest
424 error reduction (~9%) is also achieved for 120-hPa layers (dashed black line), reaching about
425 80% of the error reduction that is gained with the direct lidar height correction. The results for
426 discrete levels below the lidar cloud top (solid grey line) are less distinct. The largest error
427 reduction of about 7% is achieved for levels at 50-60 hPa (drawn in the figure at 100-120
428 hPa) below the lidar cloud top. Results for the adjusted pressure heights that are based on the
429 30-day height bias correction function are least pronounced (dashed grey line) and only show
430 a slightly positive effect (3.5% error reduction).
431

3.3 Other geostationary satellites

After demonstrating the benefit of the direct lidar height correction as well as the lidar-based bias correction for Meteosat-10-AMVs, these height correction methods are now tested for other geostationary satellites. In particular, results for GOES-AMVs and MTSAT-2-AMVs are shown for the direct lidar height correction during the first evaluation period (Fig. 10) and for the 30-day height bias correction during the second evaluation period (Fig. 11). As described in section 2.1.c, the collocation criteria for GOES-AMVs and MTSAT-2-AMVs were slightly adjusted compared to the ones applied to Meteosat-AMVs.

The mean VRMS difference and wind speed bias for the direct lidar height correction for GOES-AMVs and MTSAT-2-AMVs is illustrated in Fig. 10. Results are shown for low-level and high-level AMVs, again discarding mid-level AMVs between 400 hPa and 700 hPa. For GOES high-level AMVs (Fig. 10a), 100-120 hPa layers below the lidar cloud top show a small benefit over the operational AMV heights, with about 3% relative error reduction compared to layers of the same depth centered at the operational AMV height and 9% compared to discrete operational AMV heights. The corresponding bias values are close to zero at layer depths of approximately 80 hPa. Low-level GOES-AMVs (Fig. 10b) show a large error reduction for assigning AMVs to layers relative to the lidar cloud-top height for all layer depths, with minimum VRMS differences for 150-hPa layers. Here, the error reduction reaches 22% (30%) when these layers are compared to layers (levels) at the operational AMV height. The corresponding wind speed bias is also clearly reduced compared to the operational values. High-level AMVs from MTSAT-2 (Fig. 10c) exhibit a similar pattern as high-level GOES-AMVs, achieving lowest VRMS differences for 100 hPa deep layers below the lidar cloud top. For low-level MTSAT-2-AMVs (Fig. 10d), no distinct improvement is found for assigning AMVs to layers relative to the lidar cloud-top height

Fig. 11 shows the VRMS difference and wind speed bias for the 30-day height bias correction for GOES- and MTSAT-2-AMVs. Results for levels/layers based on a 30-day bias correction (grey bars) are compared to levels/layers relative to the operational AMV height (black bars) and relative to the lidar cloud-top height (striped bars). For high-level GOES-AMVs (Fig. 11a), the VRMS differences of the direct lidar height correction as well as the height bias correction do not show advantages over the operational height. In addition, the wind speed bias deteriorates for both height correction methods. In contrast, low-level GOES-AMVs (Fig. 11b) exhibit clearly lower VRMS differences with similarly positive results for the direct height correction and the 30-day height bias correction. Again, layer-averaging exhibits additional benefits compared to using discrete levels. High-level AMVs from MTSAT-2 (Fig. 11c) show a similar pattern as Meteosat-10-AMVs in terms of VRMS differences. Lowest values are achieved for the direct lidar height correction, but the height bias correction also leads to a small error reduction compared to the operational values. In addition, the wind speed bias is slightly reduced for both lidar height correction methods. For low-level AMVs of MTSAT-2 (Fig. 11d), the bias correction shows slightly lower VRMS differences than the operational AMV height. Wind speed bias values for both height correction methods are of similar magnitude as the operational bias.

4 Summary and conclusion

In this paper, lidar observations from the polar-orbiting satellite CALIPSO are used to correct AMV pressure heights from different geostationary satellites, with a major focus on Meteosat-10.

In the first part, results for the height correction of AMVs with directly collocated CALIPSO lidar observations are presented. In contrast to Folger and Weissmann (2014), GME model equivalents are used for the wind verification instead of radiosondes. This allows analysing a

considerably larger amount of AMVs. For Meteosat-10, both high-level and low-level AMVs exhibit lowest VRMS differences for assigning AMVs to 120-hPa deep layers below the lidar cloud top. This leads to an error reduction of 8-10% when compared to layers of the same depth centered at the operational AMV height, and about 15% when compared to the discrete operational AMV levels.

In the second part, statistical height bias corrections functions are developed based on a climatology of differences between AMV and lidar cloud-top height. Different lengths of the training period and settings for deriving the bias correction functions are tested and the resulting corrections are then applied to a subsequent verification period. This approach allows proceeding from an individual, direct height correction for a small subset of AMVs to a height adjustment of all operational AMVs from the respective geostationary satellite. Generally, adjusting AMV pressure heights of Meteosat-10 according to 30-day or 10-day height bias correction functions leads to lower VRMS differences and a lower wind speed bias compared to using the operational AMV heights. On average the reduction is about 30-50% of the reduction by the direct correction, but has the clear advantage that all AMVs can be corrected. Thereby, assigning AMVs to 120-hPa deep vertical layers relative to the adjusted heights based on a 30-day height bias correction function leads to a three times larger error reduction than assigning them to discrete levels at the mean pressure of the respective layers.

For other geostationary satellites, the positive effect of the direct lidar height correction as well as applying height bias correction functions is less distinct than for Meteosat-AMVs. However, both height correction methods overall indicate benefits in terms of VRMS differences and wind speed bias when compared to the operational wind errors. For low-level GOES-AMVs, results of the direct lidar height correction as well as of the height bias correction indicate that lidar observations can reduce wind errors by up to 30%. In contrast, high-level GOES-AMVs exhibit only small benefits for reducing VRMS differences, and

509 even show degradation in terms of the wind speed bias. This might be due to problems with
510 high-level semitransparent or multi-layer clouds. In addition, the sample size of high-level
511 GOES-AMVs is relatively small compared to low-level GOES-AMVs or AMVs from other
512 satellites. MTSAT-2-AMVs show both for high-level and low-level AMVs either neutral or
513 slightly positive effects for both lidar height correction methods when compared to results at
514 the operational AMV height.
515 The positive impact of assigning AMVs to layers instead of discrete levels shown in this
516 study coincides with findings of preceding studies (Velden and Bedka, 2009, Weissmann et
517 al., 2013). In particular, results for the model verification conducted in the present study
518 confirm the findings of the radiosonde verification shown in Folger and Weissmann (2014),
519 with lowest wind errors for 120-hPa deep layers below the lidar cloud top. This implies that
520 model error does not blur the results, therefore justifying the use of model equivalents as
521 verification also for the evaluation of the error correlation and height bias correction. Using a
522 simulated model framework, Hernandez-Carrascal and Bormann (2014) illustrated that AMVs
523 represent winds averaged over the vertical extent of a cloud instead of the cloud-top or cloud-
524 base level wind. This corresponds well to our results with lowest wind errors for assigning
525 AMVs to layers below the lidar cloud-top height.
526 This study revealed a positive impact of lidar-based height correction methods for the AMV
527 height assignment of Meteosat-AMVs, yielding lowest wind errors for the direct CALIPSO
528 lidar height correction, but still achieving a clear error reduction for the height bias correction.
529 For MTSAT-2 and GOES-AMVs, lidar height correction methods show promising results
530 especially for GOES low-level AMVs, but there is still need for research. Problems with high-
531 level GOES-AMVs for height bias correction functions could be approached by taking only
532 half of the height adjustment proposed by the respective height bias correction function. This
533 implies that both the original AMV height assignment and the lidar height correction are
534 equally weighted for assigning a new AMV height.

Overall, the direct lidar height correction has proven to be a valuable source of information for the reduction of wind errors, the wind speed bias and the error correlation of operational AMVs. As the direct lidar height correction requires collocated lidar observations for each AMV, this method is restricted to available space-borne lidar observations in real-time and therefore more complex to apply in operational data assimilation systems. The proposed height bias correction in the second part of this paper provides an alternative that does not require real-time data and is easy to implement in an NWP system. Follow-on studies to evaluate the benefit of the lidar-based height bias correction for the forecast skill of NWP models are ongoing.

In summary, this study demonstrates the potential of incorporating lidar observations into AMV height assignment methods. Space-borne lidar observations provide reliable information on cloud-top heights that is independent from the AMV processing procedures and from model fields used for the processing. The application of height correction methods based on lidar information is not restricted to CALIPSO. Other space-borne lidars are planned to be launched in the near future, e.g. the *Earth Clouds, Aerosols and Radiation Explorer* (EarthCARE, see Illingworth et al., 2014). Thus, the assimilation of AMVs as layer-averages in combination with lidar information for the AMV height correction is seen as a promising approach to increase the benefit of AMVs for NWP. Furthermore, the height bias correction with independent lidar information may be useful to derive consistent data sets for climate research and to evaluate AMV processing methods.

Acknowledgements

The operational AMV data were provided by DWD. We are grateful to Harald Anlauf and Alexander Cress from DWD for the implementation of the observation operator for the assimilation of AMVs as layer-averages in GME and their on-going support during the study.

The CALIPSO data were obtained from the NASA Langley Research Center Atmospheric Science Data Center. The study was carried out at the Hans-Ertel-Centre for Weather Research. This German research network of universities, research institutes and DWD is funded by the BMVBS (Federal Ministry of Transport, Building and Urban Development).

References

Baker, W. E., R. Atlas, C. Cardinali, A. Clement, G. D. Emmitt, B. M. Gentry, R. M. Hardesty, E. Källén, M. J. Kavaya, R. Langland, Z. Ma, M. Masutani, W. McCarty, R. B. Pierce, Z. Pu, L. P. Riishojgaard, J. Ryan, S. Tucker, M. Weissmann, and J. G. Yoe, 2013: Lidar-measured wind profiles – the missing link in the global observing system. *Bull. Amer. Meteor. Soc.*, **95**, 543–564.

Borde, R., M. Doutriaux-Boucher, G. Dew, and M. Carranza, 2014: A direct link between feature tracking and height assignment of operational EUMETSAT atmospheric motion vectors. *J. Atmos. Oceanic Technol* ., **31**, 33–46.

Bormann, N., S. Saarinen, G. Kelly, and J-N. Thépaut, 2003: The spatial structure of observation errors in atmospheric motion vectors from geostationary satellite data. *Mon. Wea. Rev.*, **131**, 706-718.

Bormann, N., and J.-N. Thépaut, 2004: Impact of MODIS polar winds in ECMWF's 4DVAR data assimilation system. *Mon. Wea. Rev.*, **132**, 929-940.

585 Bresky, W. C., J. M. Daniels, A. A. Bailey, S. T. Wanzong, 2012: New methods toward
586 minimizing the slow speed bias associated with atmospheric motion vectors. *J. Appl. Meteor.*
587 *Climatol.*, **51**, 2137–2151.
588
589 Di Michele, S., T. McNally, P. Bauer, and I. Genkova, 2012: Quality assessment of cloud-top
590 height estimates from satellite IR radiances using the CALIPSO lidar. *IEEE Trans. Geosci.*
591 *Remote Sens*., **51**, 2454-2464.
592
593 Folger, K., and M. Weissmann, 2014: Height correction of atmospheric motion vectors using
594 satellite lidar observations from CALIPSO. *J. Appl. Meteor. Climatol*., **53**, 1809-1819.
595
596 Hernandez-Carrascal, A., and N. Bormann, 2014: Atmospheric motion vectors from model
597 simulations. Part II: Interpretation as spatial and vertical averages of wind and role of clouds.
598 *J. Appl. Meteor. Climatol.,* **53**, 65–82.
599
600 Hunt, W. H, D. M. Winker, M. A. Vaughan, K. A. Powell, P. L. Lucker, and C. Weimer,
601 2009: CALIPSO lidar description and performance assessment. *J. Atmos. Oceanic Technol.*,
602 **26**, 1214-1228.
603
604 Illingworth, A. J., H. W. Barker, A. Beljaars, M. Ceccaldi, H. Chepfer, J. Cole, J. Delanoë, C.
605 Domenech, D. P. Donovan, S. Fukuda, M. Hirakata, R. J. Hogan, A. Huenerbein, P. Kollias,
606 T. Kubota, T. Nakajima, T. Y. Nakajima, T. Nishizawa, Y. Ohno, H. Okamoto, R. Oki, K.
607 Sato, M. Satoh, M. Shephard, U. Wandinger, T. Wehr, G.-J. van Zadelhoff, 2014: The
608 Earthcare satellite: The next step forward in global measurements of clouds, aerosols,
609 precipitation and radiation. *Bull. Amer. Meteor. Soc.,* accepted, doi: 10.1175/BAMS-D-12-
610 00227.1

611

612 Joo, S., J. Eyre and R. Marriott, 2013: The impact of MetOp and other satellite data within the
613 Met Office global NWP system using an adjoint-based sensitivity method. *Mon. Wea. Rev.*,
614 **141**, 3331–3342.

615

616 Lazzara, M., R Dworak, D. Santek, B. Hoover, C. Velden, and J. Key, 2014: High-latitude
617 atmospheric motion vectors from composite satellite data. *J. Appl. Meteor. Climatol*., ***53***,
618 534–547.

619

620 Salonen, K., J. Cotton, N. Bormann, and M. Forsythe, 2015: Characterizing AMV height-
621 assignment error by comparing best-fit pressures statistics from the Met Office and ECMWF
622 data assimilation systems. *J. Appl. Meteor. Climatol.*, **54**, 225–242.

623

624 Velden, C. S., J. Daniels, D. Stettner, D. Santek, J. Key, J. Dunion, K. Holmlund, G. Dengel,
625 W. Bresky, and P. Menzel, 2005: Recent innovations in deriving tropospheric winds from
626 meteorological satellites. *Bull. Amer. Meteor. Soc.*, **86**, 205-223.

627

628 Velden, C. S., and K. M. Bedka, 2009: Identifying the uncertainty in determining satellite-
629 derived atmospheric motion vector height attribution. *J. Appl. Meteor. Climatol.*, **48**, 450-463.

630

631 Weissmann, M., K. Folger, and H. Lange, 2013: Height correction of atmospheric motion
632 vectors using airborne lidar observations. *J. Appl. Meteor. Climatol*., **52**, 1868–1877.

633

634 Winker, D. M., M. A. Vaughan, A. H. Omar, Y. Hu, K. A. Powell, Z. Liu, W. H. Hunt, and S.
635 A. Young, 2009: Overview of the CALIPSO mission and CALIOP data processing
636 algorithms. *J. Atmos. Oceanic Technol*., **26**, 2310-2323.

Winker, D. M., J. Pelon, J. A. Coakley Jr., S. A. Ackerman, R. J. Charlson, P. R. Colarco, P. Flamant, Q. Fu, R. M. Hoff , C. Kittaka, T. L. Kubar, H. Le Treut, M. P. McCormick, G. Mégie, L. Poole, K. Powell, C. Trepte, M. A. Vaughan, B. A. Wielicki, 2010: The CALIPSO mission: A global 3D view of aerosols and clouds. *Bull. Amer. Meteor. Soc.*, **91**, 1211–1229.

663 **TABLES**

664

		Meteosat-10	**MTSAT-2**	**GOES (East and West comb.)**
evaluation period 1 (31 May – 11 June 2013)	high level	3673	621	226
	low level	9527	487	1192
evaluation period 2 (7 May – 12 May 2013)	high level	2144	295	143
	low level	5266	278	698

665

666

667 **TABLE 1**. Number of AMVs with collocated lidar observations used in this study for both

668 evaluation periods

669

670

671

672

673

674

675

676

677

678

679

height correction period	counts	
	low level	high level
30 days	24027	12114
30 days northern hemi.	3439	2901
30 days tropics	10889	6571
30 days southern hemi.	9699	2606
10 days	7873	4114

TABLE 2. Number of lidar-corrected AMVs used to calculate height bias correction functions over different periods for Meteosat 10. Counts of the 30-day height correction periods comprise AMVs in the period 1 Apr – 6 May 2013. Counts of the 10-day height correction period were averaged over the respective counts for each day of the 6-day evaluation period.

satellite	counts	
	low level	high level
GOES (East and West)	16005	5467
MTSAT-2	5371	7626

TABLE 3. Number of lidar-corrected AMVs used for a 30-day height bias correction function (1 Apr – 6 May 2013) for GOES and MTSAT-2.

FIGURE CAPTIONS

FIG. 1. Geographical coverage of the five main geostationary satellites and AMVs derived from these satellites with collocated CALIPSO lidar observations for the time period from 7 May 2013 to 12 May 2013.

FIG. 2. Height distribution of AMVs with collocated CALIPSO lidar observations used for (a) the direct lidar height correction (31 May 2013 – 10 June 2013) in Section 3.1 and (b) the height bias correction functions (5 May 2013 – 12 May 2013) in Section 3.2.

FIG. 3. Schematic illustration of the different layers used in this study. Layers below the lidar cloud top and layers with 25% above and 75% below the lidar cloud top are compared to reference layers centered at the operational AMV height. Layer depths vary from 0 to 200 hPa.

FIG. 4. Histogram of height differences (hPa) between original AMV pressure heights and lidar cloud-top heights for high-level and low-level AMVs combined. Positive values correspond to AMV heights that are below the respective lidar cloud top.

FIG. 5. Mean VRMS differences (upper panels) and wind speed bias (lower panels) between AMV winds and layer-averaged model winds for (a) high-level and (b) low-level Meteosat-10-AMVs. Numbers in brackets are AMV counts. Gray dashed lines represent layers centered at the original AMV pressure height; black lines represent layers below the lidar cloud-top height; black dotted lines represent layers with 25% above and 75% below the lidar cloud-top height (cf. legend).

FIG. 6. Horizontal AMV error correlations of operational AMVs (dashed black line) and lidar-corrected layer-averaged AMVs (grey line) when compared to surrounding operational AMVs for Meteosat-10 winds from all levels as a function of horizontal distance between the AMVs. The dotted line shows the number of collocations used and corresponds to the y-axis on the right.

FIG. 7. Height bias correction functions for Meteosat-10 for a 30-day period (1 April 2013 – 6 May 2013) as a function of altitude. Different line styles indicate different satellite channels (cf. legend).

FIG. 8. Mean VRMS differences (upper panels) and wind speed bias (lower panels) between AMV and model first-guess winds for (a) high-level and (b) low-level Meteosat-10-AMVs. Numbers in brackets are AMV counts. *AMV oper* corresponds to the operational AMV height, *CALIPSO* to the direct lidar height correction. Different height bias correction functions are designated as *30days* (30-day mean), *30days hemi* (30-day mean with hemispheric and tropical sub-divisions) and *10days* (10-day mean). Results are shown both for layer-averages of 120-hPa deep layers and for discrete levels.

FIG. 9. Relative reduction of VRMS differences between AMV and model winds for assigning AMVs to layers/levels below the lidar cloud top (solid lines) and to layers/levels based on the height bias correction function for a 30-day mean (grey lines) instead of the discrete operational AMV heights. Hereby, black lines represent layer-averages and grey lines discrete levels relative to the respective height. Low- and high-level AMVs are combined. The level height in hPa below the cloud top is drawn at the mean pressure of the denoted layer on the x-axis.

FIG. 10. As Fig. 3, but for (a) GOES high-level, (b) GOES low-level, (c) MTSAT-2 high-level and (d) MTSAT-2 low-level AMVs.

FIG. 11. Mean VRMS differences (upper panels) and wind speed bias (lower panels) between AMV and model winds for (a) GOES high-level, (b) GOES low-level, (c) MTSAT-2 high-level and (d) MTSAT-2 low-level AMVs. Numbers in brackets are AMV counts. *AMV oper* corresponds to the operational AMV height and *CALIPSO* to the direct lidar height correction. The applied height bias correction function is based on a 30-day mean (*30days)*. Results are shown for discrete levels and 120-hPa deep layer-averages.

FIGURES

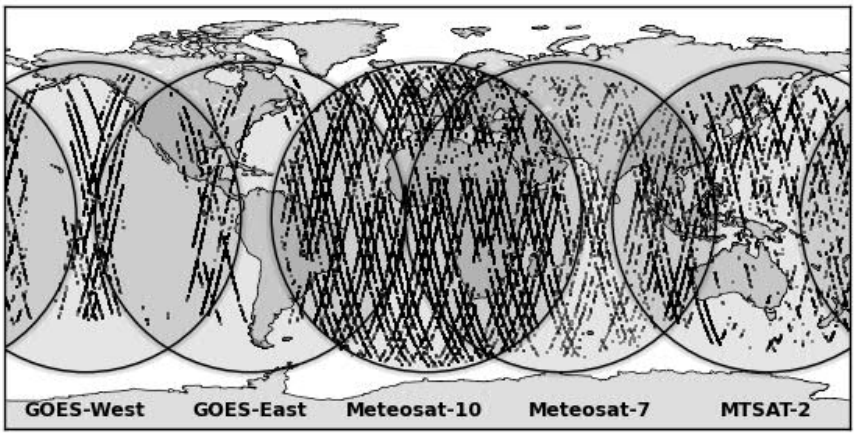

FIG. 1. Geographical coverage of the five main geostationary satellites and AMVs derived from these satellites with collocated CALIPSO lidar observations for the time period from 7 May 2013 to 12 May 2013.

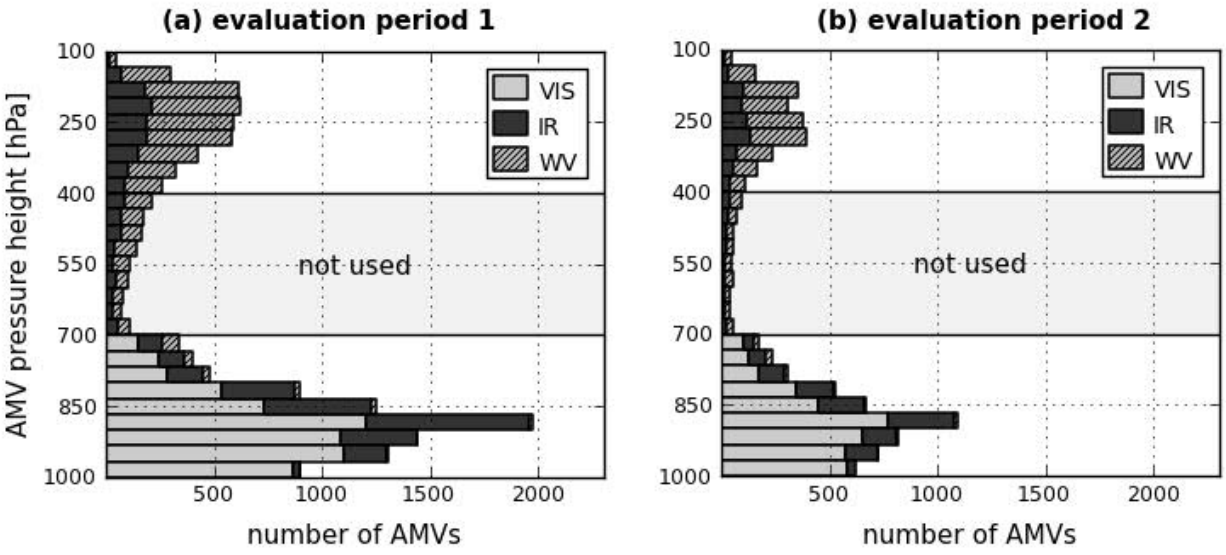

FIG. 2. Height distribution of AMVs with collocated CALIPSO lidar observations used for (a) the direct lidar height correction (31 May 2013 – 10 June 2013) in Section 3.1 and (b) the height bias correction functions (5 May 2013 – 12 May 2013) in Section 3.2.

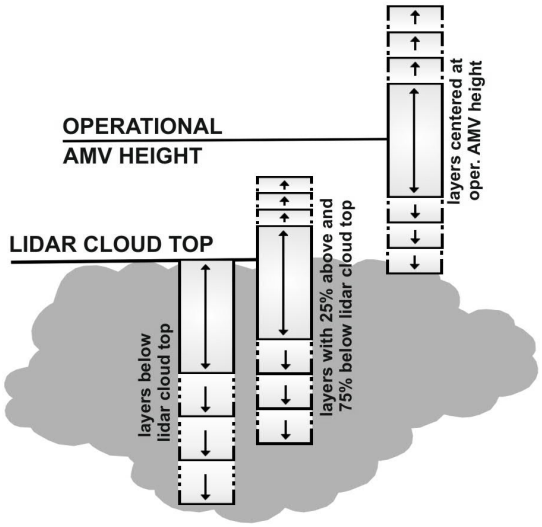

FIG. 3. Schematic illustration of the different layers used in this study. Layers below the lidar cloud top and layers with 25% above and 75% below the lidar cloud top are compared to reference layers centered at the operational AMV height. Layer depths vary from 0 to 200 hPa.

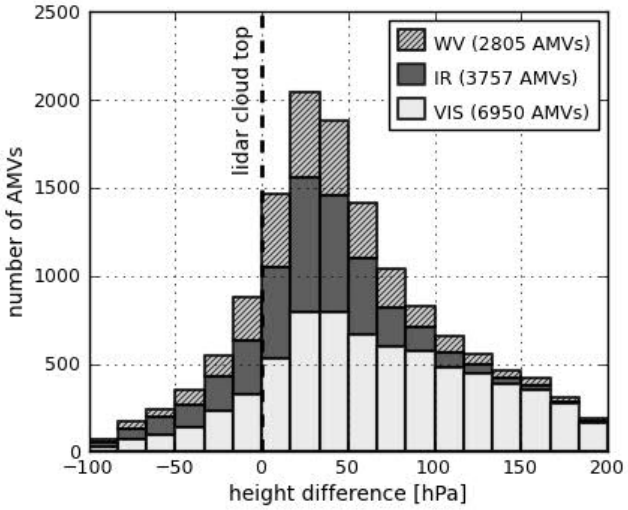

FIG. 4. Histogram of height differences (hPa) between original AMV pressure heights and lidar cloud-top heights for high-level and low-level AMVs combined. Positive values correspond to AMV heights that are below the respective lidar cloud top.

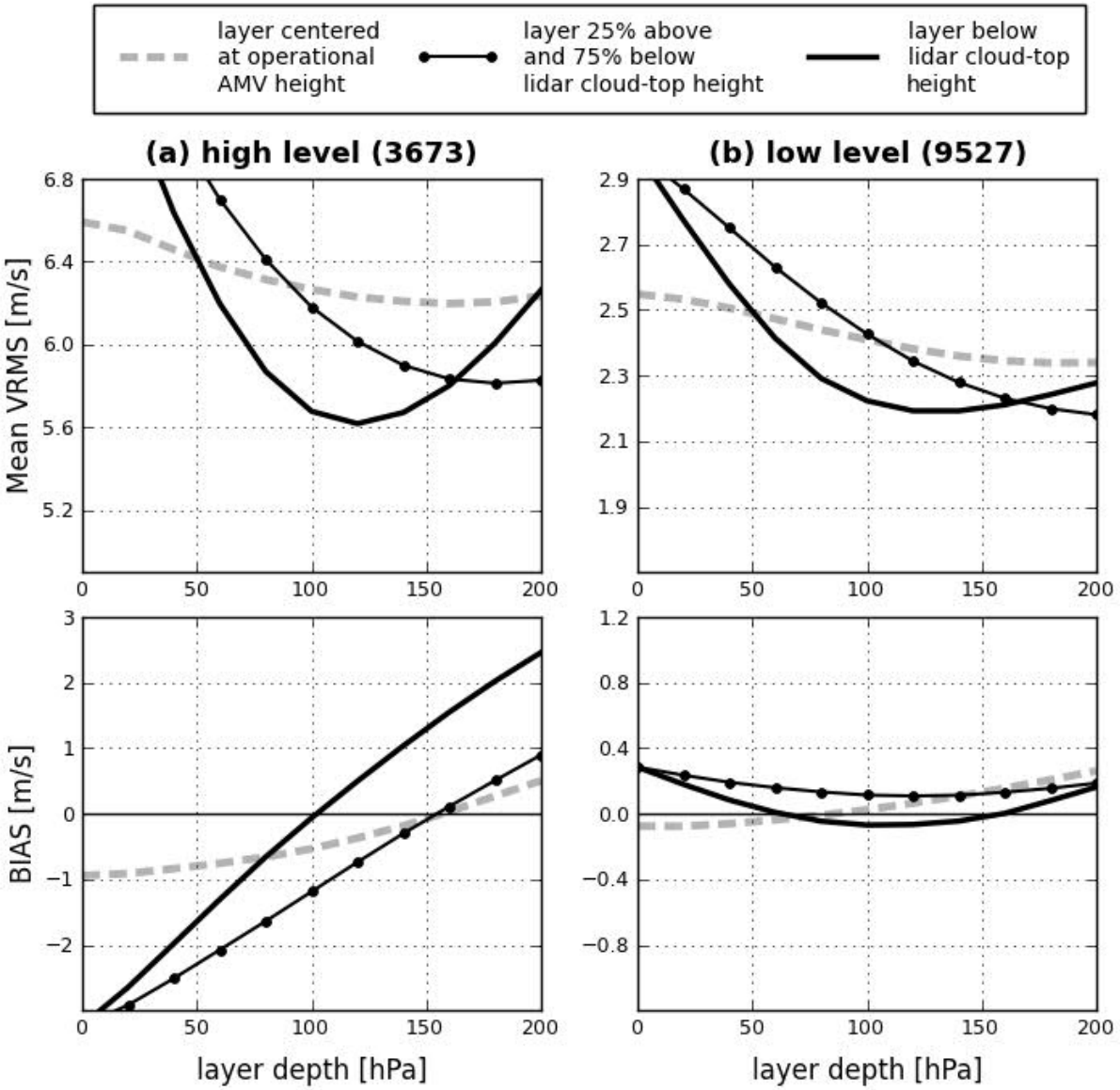

FIG. 5. Mean VRMS differences (upper panels) and wind speed bias (lower panels) between AMV winds and layer-averaged model winds for (a) high-level and (b) low-level Meteosat-10-AMVs. Numbers in brackets are AMV counts. Gray dashed lines represent layers centered at the original AMV pressure height; black lines represent layers below the lidar cloud-top height; black dotted lines represent layers with 25% above and 75% below the lidar cloud-top height (cf. legend).

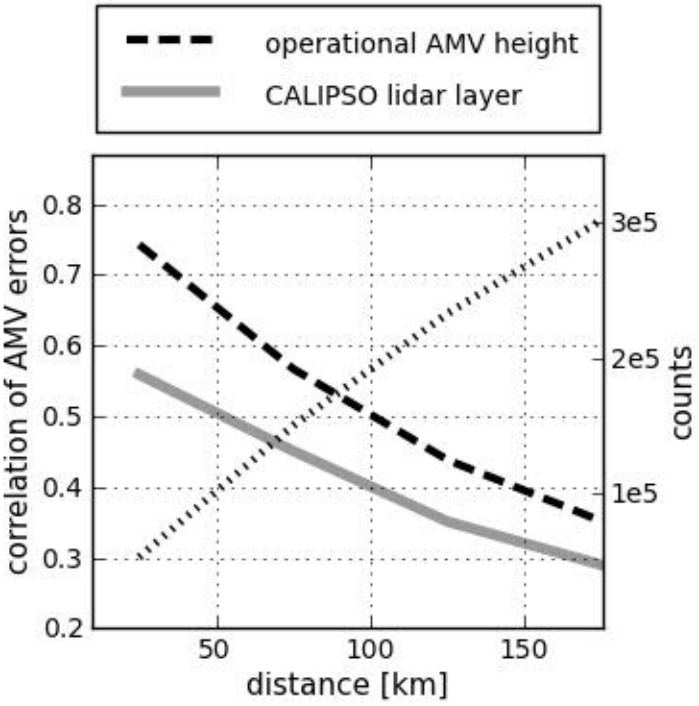

FIG. 6. Horizontal AMV error correlations of operational AMVs (dashed black line) and lidar-corrected layer-averaged AMVs (grey line) when compared to surrounding operational AMVs for Meteosat-10 winds from all levels as a function of horizontal distance between the AMVs. The dotted line shows the number of collocations used and corresponds to the y-axis on the right.

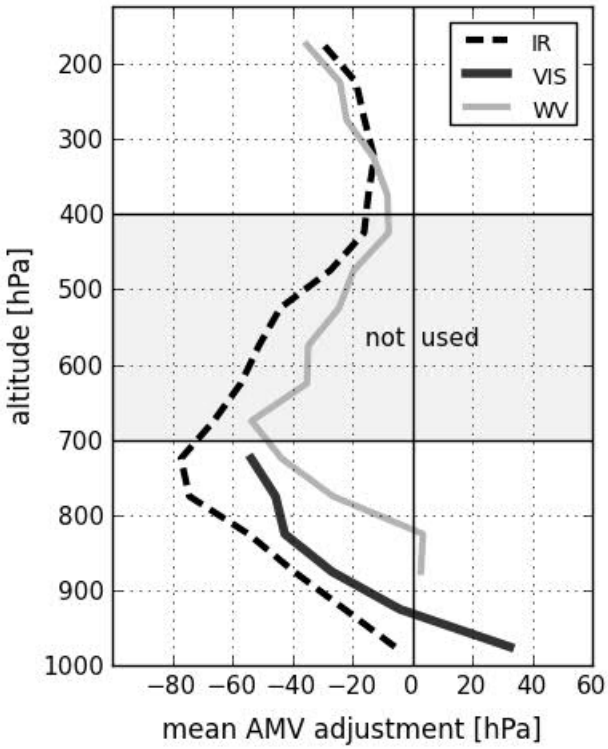

FIG. 7. Height bias correction functions for Meteosat-10 for a 30-day period (1 April 2013 – 6 May 2013) as a function of altitude. Different line styles indicate different satellite channels (cf. legend).

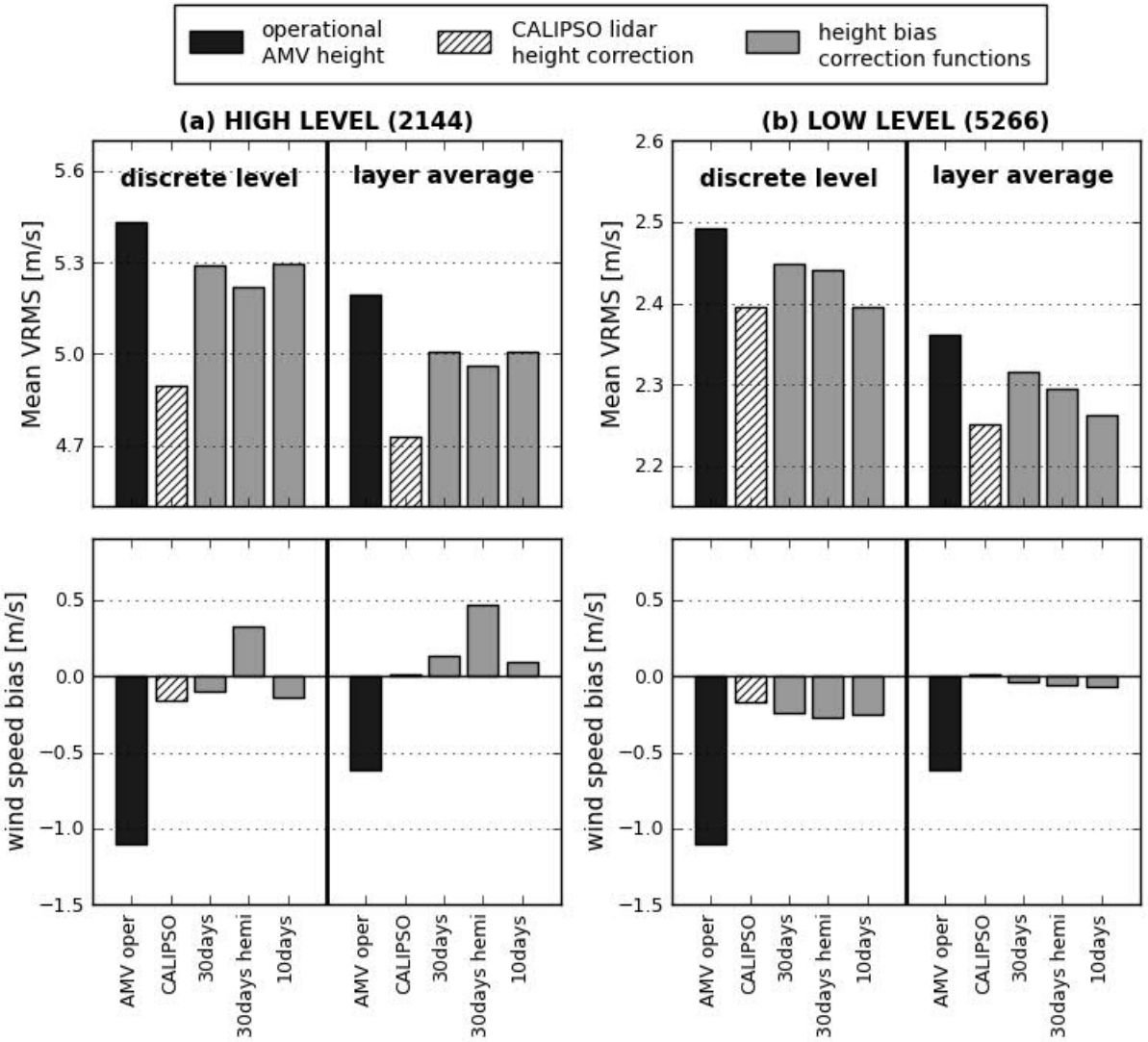

FIG. 8. Mean VRMS differences (upper panels) and wind speed bias (lower panels) between AMV and model first-guess winds for (a) high-level and (b) low-level Meteosat-10-AMVs. Numbers in brackets are AMV counts. *AMV oper* corresponds to the operational AMV height, *CALIPSO* to the direct lidar height correction. Different height bias correction functions are designated as *30days* (30-day mean), *30days hemi* (30-day mean with hemispheric and tropical sub-divisions) and *10days* (10-day mean). Results are shown both for layer-averages of 120-hPa deep layers and for discrete levels.

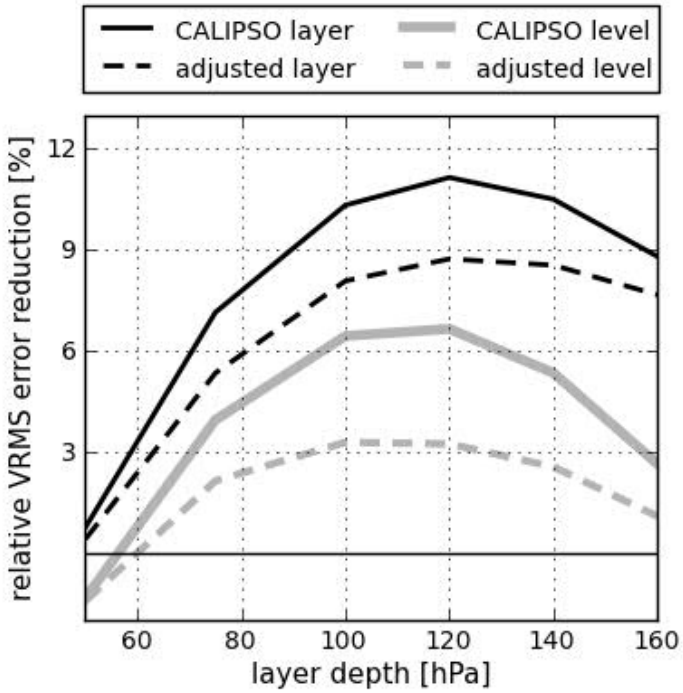

FIG. 9. Relative reduction of VRMS differences between AMV and model winds for assigning AMVs to layers/levels below the lidar cloud top (solid lines) and to layers/levels based on the height bias correction function for a 30-day mean (grey lines) instead of the discrete operational AMV heights. Hereby, black lines represent layer-averages and grey lines discrete levels relative to the respective height. Low- and high-level AMVs are combined. The level height in hPa below the cloud top is drawn at the mean pressure of the denoted layer on the x-axis.

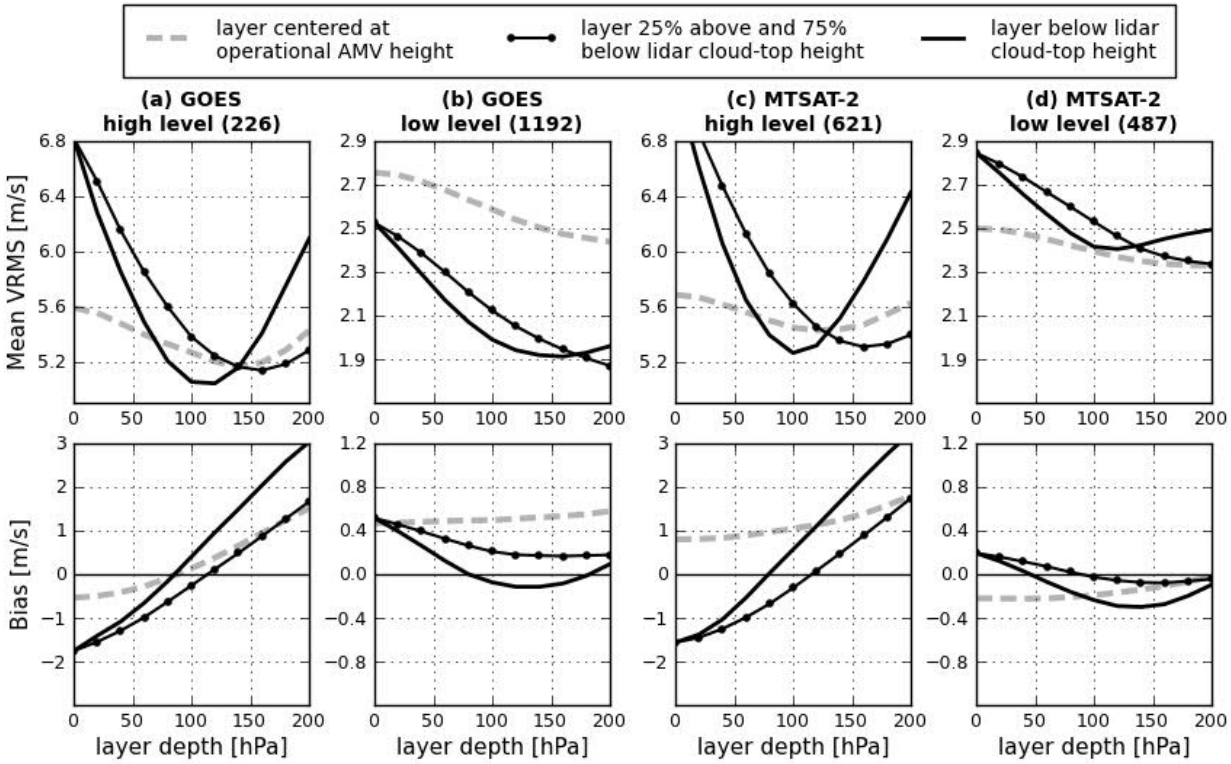

FIG. 10. As Fig. 3, but for (a) GOES high-level, (b) GOES low-level, (c) MTSAT-2 high-level and (d) MTSAT-2 low-level AMVs.

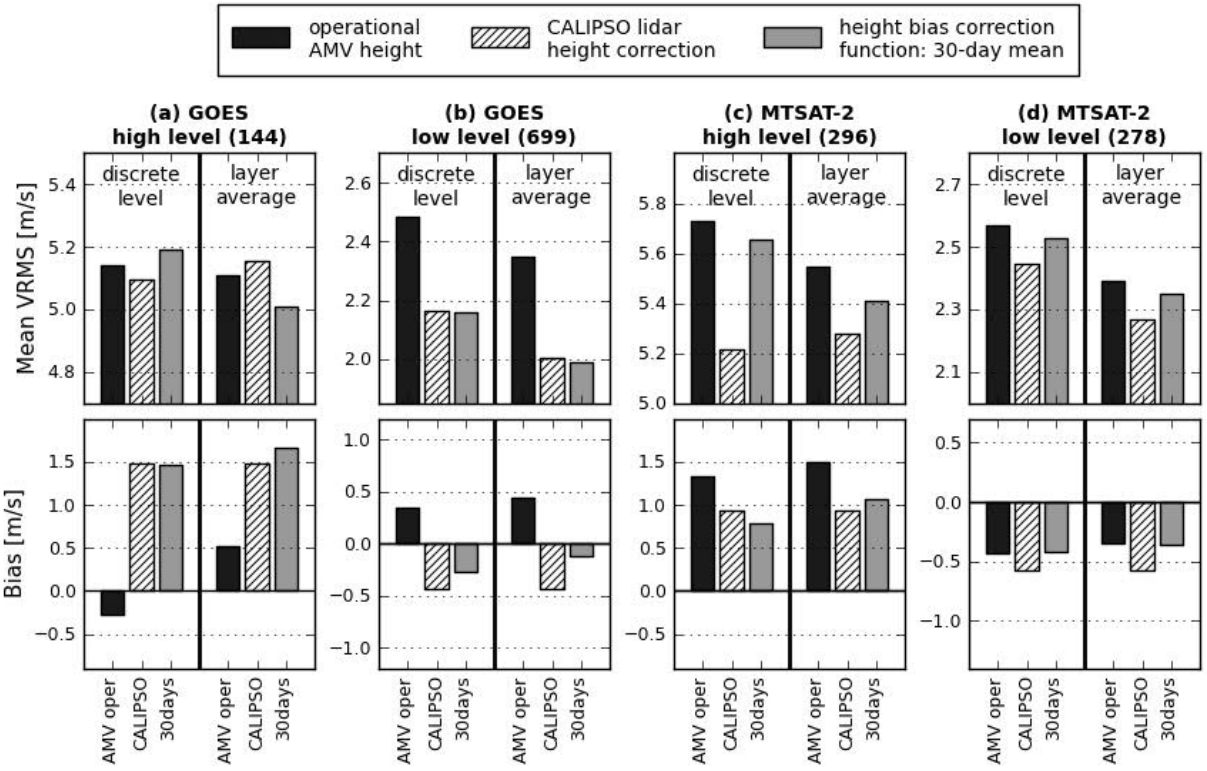

FIG. 11. Mean VRMS differences (upper panels) and wind speed bias (lower panels) between AMV and model winds for (a) GOES high-level, (b) GOES low-level, (c) MTSAT-2 high-level and (d) MTSAT-2 low-level AMVs. Numbers in brackets are AMV counts. *AMV oper* corresponds to the operational AMV height and *CALIPSO* to the direct lidar height correction. The applied height bias correction function is based on a 30-day mean (*30days)*. Results are shown for discrete levels and 120-hPa deep layer-averages.